



## OPEN Assessment of the safety of hypoxia-primed mesenchymal stem cells derived from umbilical cord and adipose tissues in animals

Nhung Thi-Hong Dinh<sup>1,4</sup>, Quyen Thi Nguyen<sup>1,4</sup>, Ngo Thu Hang<sup>3,4</sup>, Hong-Nhung Dao<sup>1</sup>, Le Duc Son<sup>1</sup>, Giang Trang Ngan<sup>1</sup>, Can Van Mao<sup>2</sup>, Xuan-Hai Do<sup>3</sup>, Van T. Hoang<sup>1</sup>✉ & Liem Nguyen Thanh<sup>1</sup>✉

Mesenchymal stem cells (MSCs) are widely used for disease treatment, typically cultured in ambient oxygen (21%) exceeding physiological levels (2–5%). While hypoxic MSCs show *in vitro* advantages, their *in vivo* effects remain less understood. This study evaluated the safety of xeno-free, serum-free cultured MSCs from adipose tissue (AD-MSCs) and umbilical cords (UC-MSCs) primed with 5% oxygen in healthy rabbits, Swiss mice, and rats. Assessments included vascular and muscle stimulation, systemic hypersensitivity, acute toxicity, and subchronic toxicity. Our data indicated that the injection of UC-MSCs induced vascular stimulation but not muscular stimulation, whereas the injection of AD-MSCs caused neither vascular nor muscular stimulation. Additionally, neither AD-MSCs nor UC-MSCs affected hematopoietic parameters (white blood cell, red blood cell, platelet, or hemoglobin levels), altered the levels of proinflammatory cytokines (IL-6, IL-1 $\beta$ , IFN- $\gamma$ , and TNF- $\alpha$ ), or induced allergic responses in rabbits. Furthermore, intravenous injection of either UC-MSCs or AD-MSCs at a dose of  $50 \times 10^6$  cells/kg did not cause acute toxicity in mice. However, injections of higher doses of these cells led to intravenous thrombosis and embolism in various organs of experimental animals, ultimately resulting in animal death. Finally, according to the subchronic toxicity assay, the administration of MSCs generally did not impact liver, kidney, or spleen function in rats. In conclusion, hypoxic AD-MSCs and UC-MSCs are safe for potential therapeutic use with consideration of thrombotic risk. We suggest that these hypoxic MSC lines could be alternatives to normoxic MSCs for disease treatment.

**Keywords** Mesenchymal stem cells, Hypoxia preconditioning, Safety evaluation, Vascular stimulation, Muscle stimulation, Systemic hypersensitivity, Toxicity

Mesenchymal stem cells (MSCs) are multipotent adult stem cells that can differentiate into various cell types, including osteoblasts, chondrocytes, adipocytes, and fibroblasts<sup>1,2</sup>. Although MSCs are found in various tissues, bone marrow (BM), adipose tissue (AD), and the umbilical cord (UC) are considered the most common clinical sources of MSCs<sup>3–5</sup>. MSCs have attracted significant attention in biomedical research and regenerative medicine because of their unique properties, including modulating immune responses, secreting growth factors, and releasing extracellular vesicles that support cell growth, survival, and neovascularization<sup>6</sup>. MSCs are valuable and easily accessible, and they play crucial roles in cell therapy for tissue repair, regeneration, and the treatment of immune-related conditions, including autoimmune diseases and graft-versus-host disease (GVHD) in transplant patients<sup>6–8</sup>.

Although MSCs are typically cultured under conditions with ambient oxygen levels (21% oxygen), many studies have demonstrated that their biological activity increases under hypoxic conditions<sup>9,10</sup>. Priming MSCs under hypoxic culture conditions involves exposing them to low oxygen concentrations, usually ranging from 2% to 9% O<sub>2</sub><sup>11</sup>. The scientific rationale of hypoxic culture is that the physiological microenvironments of many

<sup>1</sup>Vinmec Research Institute of Stem Cell and Gene Technology, College of Health Science, VinUniversity, Vinhomes Ocean Park, Gia Lam 12400, Hanoi, Vietnam. <sup>2</sup>Department of Pathophysiology, Vietnam Military Medical University, 160 Phung Hung, Ha Dong, Hanoi, Vietnam. <sup>3</sup>Department of Practical and Experimental Surgery, Vietnam Military Medical University, 160 Phung Hung, Ha Dong, Hanoi, Vietnam. <sup>4</sup>These authors contributed equally to this work: Nhung Thi-Hong Dinh, Quyen Thi Nguyen and Ngo Thu Hang. ✉email: v.vanht8@vinmec.com; v.liemnt@vinmec.com

tissues in the human body are characterized by hypoxia<sup>9,10</sup>. For example, the normal oxygen concentration in the BM is between 1% in the hypoxic niche and 6% in the sinusoidal cavity, the normal oxygen concentration in AD is between 2% and 8%, and the normal oxygen concentration in the placenta is between 2% and 3%<sup>12–15</sup>. Culturing MSCs under hypoxic conditions could expose the cells to conditions that mimic the in vivo environment prior to their introduction into target tissues, thus supporting cell proliferation at the target site<sup>16–18</sup>. Furthermore, priming MSCs under hypoxic conditions helps preserve their stemness<sup>17</sup> and stimulates them to secrete various cytokines and growth factors that promote angiogenesis<sup>19–21</sup>. Moreover, hypoxia can influence the immunomodulatory properties of MSCs<sup>22–24</sup>. Culturing MSCs under hypoxic conditions has been shown to increase their therapeutic efficacy in preclinical models<sup>25</sup>, including cerebral ischemia in rats<sup>26</sup>, liver cirrhosis in mice<sup>27</sup>, pulmonary fibrosis in mice<sup>28</sup>, and lung injuries in rats<sup>29</sup>. These findings suggest that hypoxia-primed MSCs may have greater potential for clinical translation.

Fetal bovine serum (FBS) supports robust cell growth but raises concerns about pathogen contamination, animal-derived components, and batch-to-batch variability<sup>30</sup>. Serum-free and xeno-free (SF/XF) media have been developed as alternatives to FBS-supplemented media<sup>31</sup>. Our group previously established a standardized SF/XF platform for producing high-quality MSCs for research and clinical use<sup>32</sup>. While hypoxic MSCs cultured in FBS-based media have been well-studied in vitro, their safety in SF/XF conditions in animal models remains unclear. In this study, we evaluated the safety of hypoxic AD-MSCs and UC-MSCs, cultured in SF/XF condition under 5% oxygen, in healthy rabbits, Swiss mice, and rats. This proof-of-concept study provides an important safety data supporting the potential of hypoxia-primed MSCs as a therapeutic strategy for various diseases.

## Materials and methods

### Isolation of AD-MSCs and UC-MSCs

UC-MSCs and AD-MSCs were isolated from umbilical cord and adipose tissues collected during cesarean delivery. The donor was a healthy 35-year-old pregnant woman who provided written informed consent. Adipose tissue was obtained from the subcutaneous layer at the abdominal incision site. The umbilical cord was collected immediately after delivery. The method for cell isolation was previously described<sup>32</sup>. Briefly, the tissues were cut into small fragments and incubated in 500 U/ml collagenase type I (Sigma, Germany). The isolated cells were plated at 3,200 cells/cm<sup>2</sup> in culture flasks that were coated with CTS™ CELLstart™ substrate (Gibco, USA). Primary cells were cultured in StemMACS™ MSC Expansion Media (Miltenyi Biotec, Germany) under SF/XF conditions at 95% Humidity at 37 °C with 5% CO<sub>2</sub> with ambient oxygen levels (21% oxygen). MSCs were harvested when they reached 80% confluence. For long-term storage, the MSCs were cryopreserved with CryoStorR CS10 (Stemcell Technologies, Singapore) in vapor-phase liquid nitrogen. The temperature was monitored and maintained at –196 °C. Sample collection and data analysis were approved by the Ethics Council of Vinmec International Hospital (No.03/2022/QĐ-VNC). All methods were performed in accordance with the relevant guidelines and regulations.

### Cell culture and characterization

Cryopreserved AD-MSCs and UC-MSCs were thawed and cultured in StemMACS™ MSC Expansion Media (Miltenyi Biotec, Germany) at 37 °C with 5% CO<sub>2</sub> and 21% O<sub>2</sub> at a density of 3,200 cells/cm<sup>2</sup> in a T225 culture flask (Thermo Scientific, USA) until passage 5. When the MSCs reached passage 6, they were grown in a hyperflask (Corning, USA) in 21% oxygen for 3 days; then, they were moved to hypoxic conditions with 5% oxygen and cultured for 2 days. When the MSCs reached confluence, they were harvested using TrypLE Select CTS enzyme (Gibco, USA) and characterized before being stored in liquid nitrogen at –196 °C for further experiments. For the animal experiments, cells were resuspended in Ringer's lactate solution prior to administration.

To analyze MSC surface marker expression, the harvested AD-MSCs and UC-MSCs were stained with antibodies against positive markers (CD90 FITC, CD105 PerCP-Cy5.5, and CD73 APC) and a cocktail of antibodies against negative marker (CD45/CD34/CD11b/CD19/HLA-DR PE) via a BD Stemflow™ Human MSC Analysis Kit (BD, Biosciences, USA) according to the manufacturer's instructions. Human MSC Isotype Control Negative Cocktail and human MSC Isotype Control Positive Cocktail (BD Biosciences, USA) were used as isotype controls. The stained cells were analyzed with a MACSQuant® Analyzer 10 flow cytometer, and the data were analyzed via FlowJo software. Furthermore, the differentiation potential of UC-MSCs and AD-MSCs into osteoblast and chondrocyte and adipocyte were investigated using StemPro™ osteogenesis differentiation medium, chondrogenesis differentiation medium and adipocyte differentiation kit (Gibco, USA), respectively, and were visualized under a bright-field microscope. Sterility of the cells were confirmed by the absence of bacteria, fungi, and mycoplasma. All the tests were carried out at the Quality Control facility at the HiTech Center of Vinmec International Hospital (Vietnam).

### Animals

All animals were purchased from Le Thi Mo business households (Business License No. 01S8001565 issued by Department of Finance and Planning – People's Committee, Hanoi, Vietnam). The work has been reported in accordance with ARRIVE guidelines 2.0. The safety study was conducted using Wistar rats (200–300 g, 12–14 weeks old), Swiss mice (20–30 g, 6–8 weeks old), and New Zealand white rabbits (1.8–2 kg, 4–4.5 months old). The animals were maintained under conditions with a 12-h light/dark cycle and free access to food and water at the facility of Vietnam Military Medical University. All animal procedures were conducted in accordance with the guidelines of the Institutional Review Board (IRB) for Animal Experiments. The experimental protocols were approved by the IRB of the Dinh Tien Hoang Institute of Medicine, Vietnam (Approval No. IRB-A-2201).

### Evaluation of vascular and muscle stimulation by MSCs in rabbits

New Zealand white rabbits (4–4.5 month old, total 21 animals) were randomly divided into 5 groups ( $n = 7$  per group). The evaluation followed a method described in a previous publication<sup>33</sup>. For the vascular stimulation test, rabbits were intravenously injected through the ear marginal vein with AD-MSCs or UC-MSCs at  $0.5 \times 10^6$  cells/kg. For the muscle stimulation test, the animals received the same dose of AD-MSCs or UC-MSCs intramuscularly into the right quadriceps muscle. The group that was injected with Ringer's lactate served as a control. The temperature at the injection sites was recorded daily. The animals were sacrificed on day 4 postinjection, and the local tissues surrounding the injection sites were collected. These tissues were fixed in 4% paraformaldehyde, embedded in paraffin, and sectioned into 5- $\mu\text{m}$ -thick slices. These sections were then subjected to hematoxylin and eosin (HE) staining and imaged via a microscope (Olympus, Japan) for histological analysis.

To analyze the vessels, images of HE-stained samples were captured with a 4X objective lens, and the vessel diameter was measured. The percentage of blood vessel area was determined by calculating the percentage of blood vessel area per 4X field area (equivalent to  $4,576,000 \mu\text{m}^2$ ). The vessel density was determined by calculating the average number of blood vessels per  $\text{mm}^2$  of the HE images as captured with a 20X objective lens. The percentage of the lesion area was calculated as the percentage of the lesion area in each 4X field area. Representative lesion areas were selected, and images were captured with a 20X objective lens to calculate the number of white blood cells (WBCs). All the image analyses were conducted with OPTIKA Proview software. To analyze the muscle samples, the blood vessel diameter and area were measured in HE images that were captured with a 10X objective lens. The percentage of blood vessel area was calculated on the basis of the percentage of blood vessel area per 10X field area (equivalent to  $729,600 \mu\text{m}^2$ ).

### Evaluation of systemic hypersensitivity in rabbits

New Zealand white rabbits (1.8–2 kg, 4–4.5 month old, total 17 animals) were randomly divided into 5 groups ( $n = 3$ –5 per group). The animals received repeated injections of UC-MSCs or AD-MSCs via the ear marginal vein at low doses ( $0.125 \times 10^6$  cells/kg) or high doses ( $2.5 \times 10^6$  cells/kg) on days 0, 2, and 4. On day 14, each received double the initially administered doses ( $0.25 \times 10^6$  or  $5 \times 10^6$  cells/kg). Animals that were injected with Ringer's lactate served as controls. The body weights and temperatures of the animals were monitored for 14 days. Blood samples were collected before injection; at 2 days after the 1st, 2nd, and 3rd injections; and at 8 days after the 4th injection. Hematological parameters (RBC count, WBC count, platelet count, and hemoglobin level) were analyzed. Plasma allogenic cytokine (histamine and IgE) and systemic proinflammatory cytokine (IL-6, IL-1 $\beta$ , IFN- $\gamma$ , and TNF- $\alpha$ ) levels were measured with ELISA kits following the manufacturer's instructions. The ELISA kits that were utilized in this study included a rabbit IL-1 beta ELISA kit (ER5RB; Invitrogen, USA), a rabbit IL-6 ELISA kit (ab277389; Abcam, UK), a rabbit IFN-gamma ELISA kit (ab273238; Abcam, UK), a rabbit TNF alpha ELISA kit (ab236712; Abcam, UK), a histamine ELISA kit (ab285333; Abcam, UK), and a rabbit IgE ELISA kit (ab287818; Abcam, UK).

### Evaluation of acute toxicity in mice

Swiss mice (28–30 g, 6–8 week old, total 60 animals) were randomly divided into 10 groups ( $n = 6$  in each group). Different doses (50, 200, 500, and  $1000 \times 10^6$  cells/kg) of UC-MSCs or AD-MSCs were intravenously injected into the animals. Ringer's lactate served as the negative control. The body weights and mortality rates were monitored daily for 14 days. The median lethal dose (LD50), the dose that caused death in 50% of the tested animals after MSC administration, was determined via the Miller–Tainter method<sup>37</sup>.

### Subchronic toxicity test in rats

Wistar white rats (200–300 g, 12–14 week old, 36 animals) were randomly divided into 6 groups ( $n = 6$  in each group). The mice received three intravenous injections of either UC-MSCs or AD-MSCs ( $5 \times 10^6$  cells/kg (low dose) or  $15 \times 10^6$  cells/kg (high dose)) via the tail at 10-day intervals. The groups injected with Ringer's lactate were used as controls. The physical conditions of the animals (body weight, food consumption, diarrhea, abnormal behaviors, and mortality) were recorded until day 29 of the experiment. Blood was collected on day 0 and after each injection, and hematological indices, including WBC, RBC, platelet, and hemoglobin levels, were determined. Serum levels of urea, creatinine, AST, and ALT were measured on day 0 and after each injection to assess liver and kidney damage. On day 10 after the final injection, H&E staining was used to assess the histology of the liver, kidney, and spleen.

### Euthanasia method

Animals were first anesthetized with 5% isoflurane in oxygen at a flow rate of 1 L/min to induce unconsciousness. Once fully anesthetized, they received an intraperitoneal injection of pentobarbital sodium (100 mg/kg) to cause permanent loss of vital functions. Death was confirmed by the absence of heartbeat and breathing before continuing with further experimental steps.

### Statistical analysis

The data were presented as the means  $\pm$  standard deviation (SD). Statistical significance was analyzed by unpaired t test or one-way ANOVA with GraphPad Prism 8.4.3 software.  $p \leq 0.05$  was considered statistically significant.

## Results

### Isolation and characterization of AD-MSCs and UC-MSCs

The morphology, surface marker expression, and differentiation potential of the isolated MSCs were characterized. We found that both AD-MSCs and UC-MSCs exhibited a spindle-like shape with fibroblast characteristics (Fig. 1A). More than 95% of the cell population expressed positive markers (CD73, CD90, and CD105) and

fewer than 2% of the population expressed negative markers (CD45/CD34/CD11b/CD19/HLA) (Fig. 1B). Both AD-MSCs and UC-MSCs successfully differentiated into 3 lineages, including osteoblasts, chondrocytes, and adipocytes (Fig. 1C). Together, our data demonstrated that both hypoxic UC-MSCs and AD-MSCs fully met the

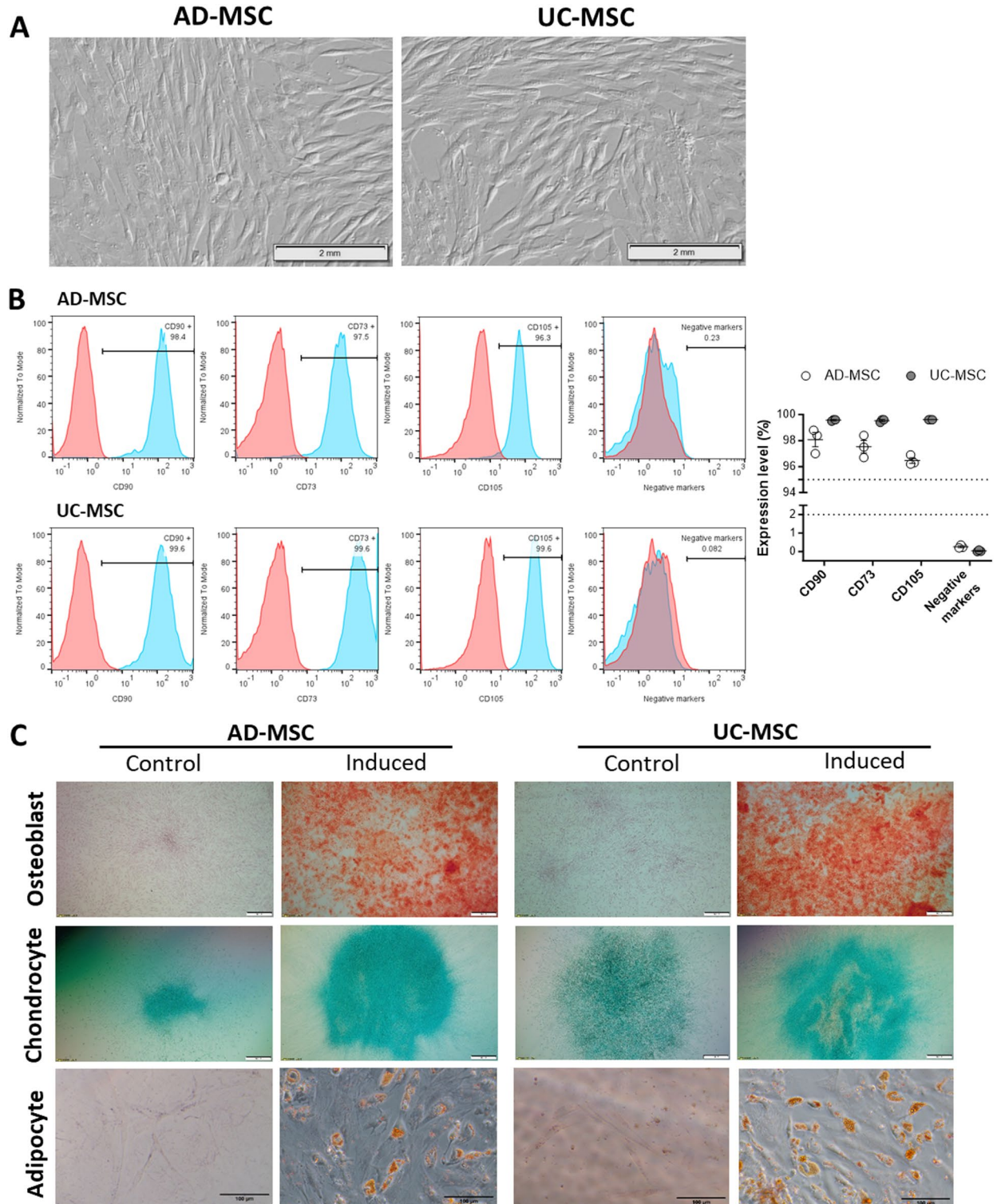


**Fig. 1.** Characterization of hypoxic UC-MSCs and AD-MSCs. **(A)** Cellular morphology of UC-MSCs and AD-MSCs under hypoxic conditions with 5% oxygen (scale bar, 2 mm). **(B)** Analysis of MSC marker expression by flow cytometry. **(C)** Differentiation ability of MSCs into osteoblasts (scale bar, 500  $\mu$ m), chondrocytes (scale bar, 500  $\mu$ m), and adipocytes (scale bar, 100  $\mu$ m) via bright-field microscopy.

criteria for defining MSCs of the International Society for Cell and Gene Therapy (ISCT)<sup>34</sup>. Moreover, all cell preparations tested negative for bacteria, fungi, and mycoplasma contamination.

### Vascular or muscle stimulation by UC-MSCs and AD-MSCs in rabbits

To evaluate vascular stimulation by UC-MSCs and AD-MSCs, rabbits were injected with  $0.5 \times 10^6$  cells/kg via the ear marginal vein. After injection, 2/7 rabbits in the UC-MSC group exhibited swelling and redness in the injected ear at 24 h, with symptoms resolving in 1/7 by 96 h. No such changes were observed in other groups. Ear temperature was recorded before injection and at 30 min, 24 h, 48 h, 72 h, and 96 h postinjection, with no significant differences observed between pre- and postinjection in any group (Fig. 2A). HE staining of injected ear tissue collected at 96 h postinjection did not reveal any significant differences in vessel density (Fig. 2B), vessel diameter (Fig. 2C), or vessel area (Fig. 2D) between the MSC-injected groups and the control group. While the percentage of lesion area (Fig. 2E) and the number of WBCs per  $\text{mm}^2$  (Fig. 2F) were significantly greater in the UC-MSC group than in the control group ( $p < 0.05$ ), these parameters were not significantly different between the AD-MSC group and the control. No noticeable changes were observed in the gross ear structure of MSC-treated groups or the control group when examined in low-magnification HE images (Fig. 2G, top). However, higher-magnification views revealed differences in the number of infiltrating cells among groups. Both UC-MSC and AD-MSC groups showed increased cell infiltration compared with the control group, but the increase was statistically significant only in the UC-MSC group (Fig. 2G, bottom). These findings suggest that UC-MSC treatment induces localized inflammation at the injection site.

To investigate muscle stimulation by UC-MSCs and AD-MSCs, rabbits were injected with  $0.5 \times 10^6$  cells/kg via the right quadriceps muscle. No symptoms of bleeding, edema, necrosis, or mild hemorrhage were observed at the injection site in the rabbit muscle after injection with either UC-MSCs or AD-MSCs. Compared with that at baseline, the muscle temperature of both MSC-injected groups slightly increased at 24 h after injection and then returned to the normal level. Overall, the muscle temperature was comparable between the control and MSC-injected groups at all the analyzed time points (Fig. 2H). Similarly, the diameter of the blood vessels (Fig. 2I) and the blood vessel area (Fig. 2J) of the MSC-treated muscles did not differ from those of the Ringer's lactate-injected muscles.

Collectively, our data indicates that while the injection of AD-MSCs causes no vascular stimulation, UC-MSCs can induce vascular stimulation in rabbits, as shown by the development of swelling and redness and the increase in the number of WBCs and lesion areas in the tissues of injected animals. Neither AD-MSCs nor UC-MSCs cause muscular stimulation.

### Systemic hypersensitivity of rabbits to UC-MSCs and AD-MSCs

To investigate whether MSCs trigger systemic hypersensitivity, rabbits were administered UC-MSCs or AD-MSCs at a dose of 0.125 or  $2.5 \times 10^6$  cells/kg on days 0, 2, and 4 and an additional double dose of MSCs (0.25 or  $5 \times 10^6$  cells/kg) on day 14. The control group received injections of Ringer's lactate (Fig. 3A). Body weight gradually increased in all five experimental groups to a comparable degree ( $p > 0.05$ ) (Fig. 3B). Although there were minor fluctuations in the body temperature of the animals in all the groups after injection, these changes did not significantly differ among the groups (Fig. 3C). Similarly, there were no significant differences in the levels of RBCs, hemoglobin, and WBCs in the rabbits between the injected groups and the control group ( $p > 0.05$ ) (Fig. 3D-F). However, the platelet count was lower in the groups that were treated with high doses of AD-MSCs and UC-MSCs than in the groups that were treated with low doses ( $p < 0.05$ ) (Fig. 3G). Importantly, 2/7 rabbits in the UC-MSC-high group died (one following each of the 1st and 2nd injections) and 3/7 animals in the AD-MSC-high group died (one following the 3rd injection and the others following the 4th injection). Autopsy revealed small blood clots in the lungs of the deceased rabbits (Fig. 3H).

Next, the levels of allergy-related cytokines (histamine and IgE) and proinflammatory cytokines (IL-6, IL-1 $\beta$ , IFN- $\gamma$ , and TNF- $\alpha$ ) in the plasma of the injected animals were measured. In general, no significant changes in the levels of the measured cytokines were detected in either the UC-MSC- or AD-MSC-injected group or the control group (Fig. 4A-F). Nevertheless, the histamine concentration of the AD-MSC-high group after the 3rd injection was significantly greater than that before and after the 1st injection ( $p < 0.05$ ) (Fig. 4A). Similarly, the IL-1 $\beta$  plasma level was increased in the AD-MSC-high group after the 4th injection compared to the levels at earlier time points ( $p < 0.05$ ) (Fig. 4E). The plasma IFN- $\gamma$  concentration was greater in the AD-MSC-high group after the 4th injection than after the 2nd injection ( $p < 0.05$ ) (Fig. 4F). In general, although the platelet number and cytokine concentration fluctuated between the high-dose and low-dose MSC-injected groups, as well as between the pre- and post-injection measurements, neither UC-MSCs nor AD-MSCs affected the physical conditions, hematopoietic function, systemic allergy, or immune response of the tested rabbits.

### Acute toxicity of UC-MSCs and AD-MSCs

To determine the acute toxicity of MSCs, mice were injected with UC-MSCs or AD-MSCs at escalating doses of 50, 200, 500, or  $1000 \times 10^6$  cells/kg or with Ringer's lactate ( $n = 6$  per group). The body weights and mortality rates of the injected animals were monitored for 14 days after injection (Fig. 5A). After the injection of UC- and AD-MSCs, the body weights of the mice gradually increased (Fig. 5B and D). In the groups that were injected with UC-MSCs, 2/6 (33.3%), 2/6 (33.3%), and 4/6 (66.7%) of the mice died when injected with doses of  $200 \times 10^6$ ,  $500 \times 10^6$ , and  $1000 \times 10^6$  cells/kg, respectively (Fig. 5C). The injection of AD-MSCs caused the death of 2/6 (33.3%), 1/6 (16.7%), and 3/6 (50%) of the mice in the groups that were injected with the corresponding doses of  $200 \times 10^6$ ,  $500 \times 10^6$ , and  $1000 \times 10^6$  cells/kg, respectively (Fig. 5E). To calculate LD50 values, mortality rates of each experimental group were converted to probit values via Finney's table (Suppl. Table S1). A linear regression curve of the probit values and logarithmic values of the injected doses was established for UC-MSC (Suppl.

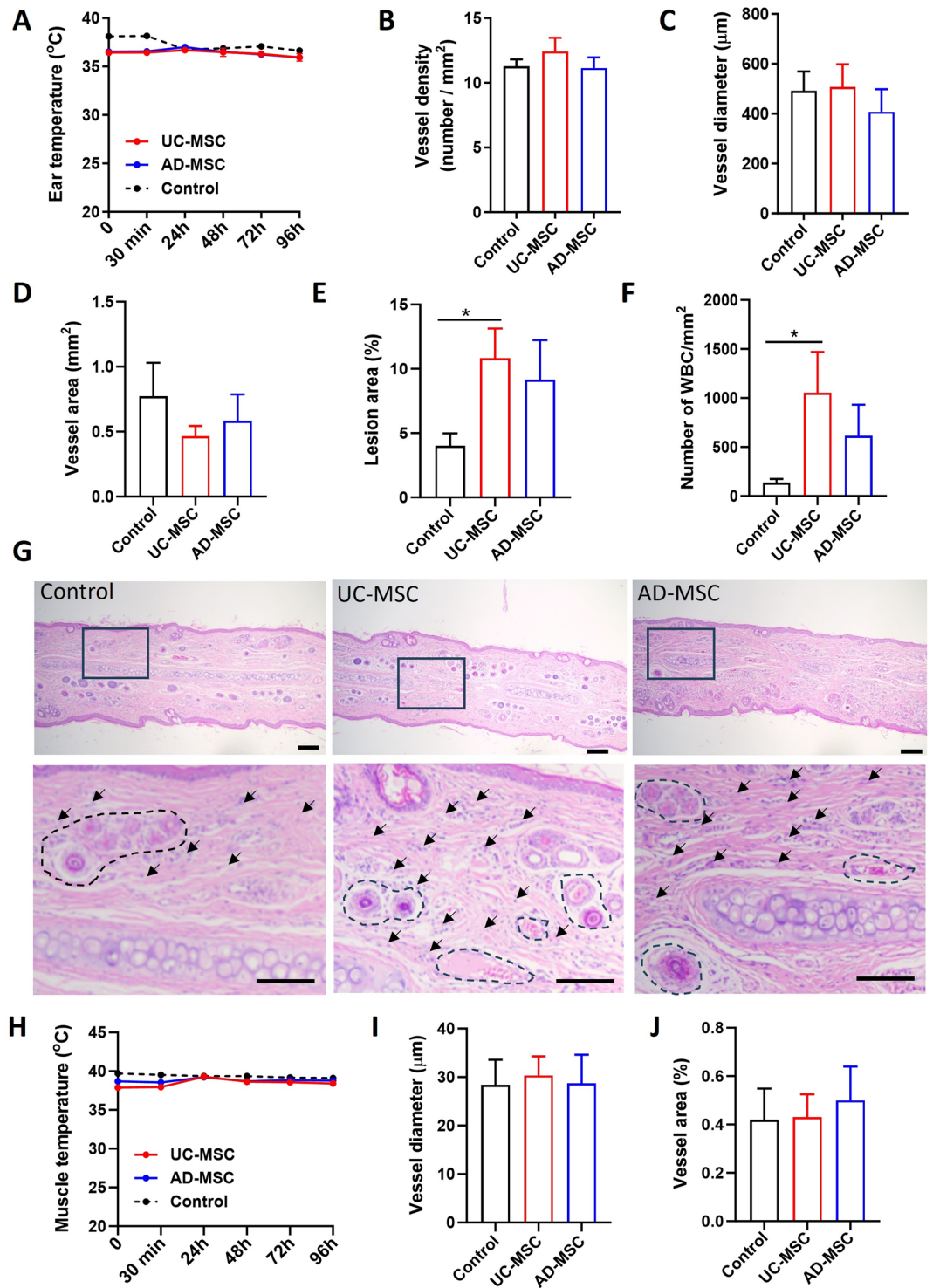


**Fig. 2.** Vascular and muscle stimulation testing of UC-MSCs and AD-MSCs in rabbits. New Zealand rabbits ( $n = 7$ ) were injected with  $0.5 \times 10^6$  cells/kg of UC-MSCs or AD-MSCs. The group that was injected with Ringer's lactate served as the control. (A–F) Evaluation of vascular stimulation. Ear temperature was measured at the indicated time points (A). Analysis of the HE-stained injected ear tissues at 96 h after injection to determine the number of blood vessels per mm<sup>2</sup> (B), blood vessel diameter (C), blood vessel area (D), percentage of lesion area (E), number of WBCs (F). (G) Representative H&E-stained sections of ear tissue. The top panels showed low-magnification views (scale bar, 50 μm), with boxed areas indicating regions enlarged below. The bottom panels (scale bar, 25 μm) presented higher-magnification views of the corresponding boxed areas. Dashed lines outlined blood vessels, and black arrows indicated infiltrating cells. (H–K) Evaluation of muscle stimulation. The muscle temperature was recorded at the indicated time points (H). HE-stained muscle samples were analyzed at 96 h after injection to measure the blood vessel diameter (I) and blood vessel area (J). Data were presented as mean  $\pm$  SD; \*,  $p < 0.05$  as determined by t test.

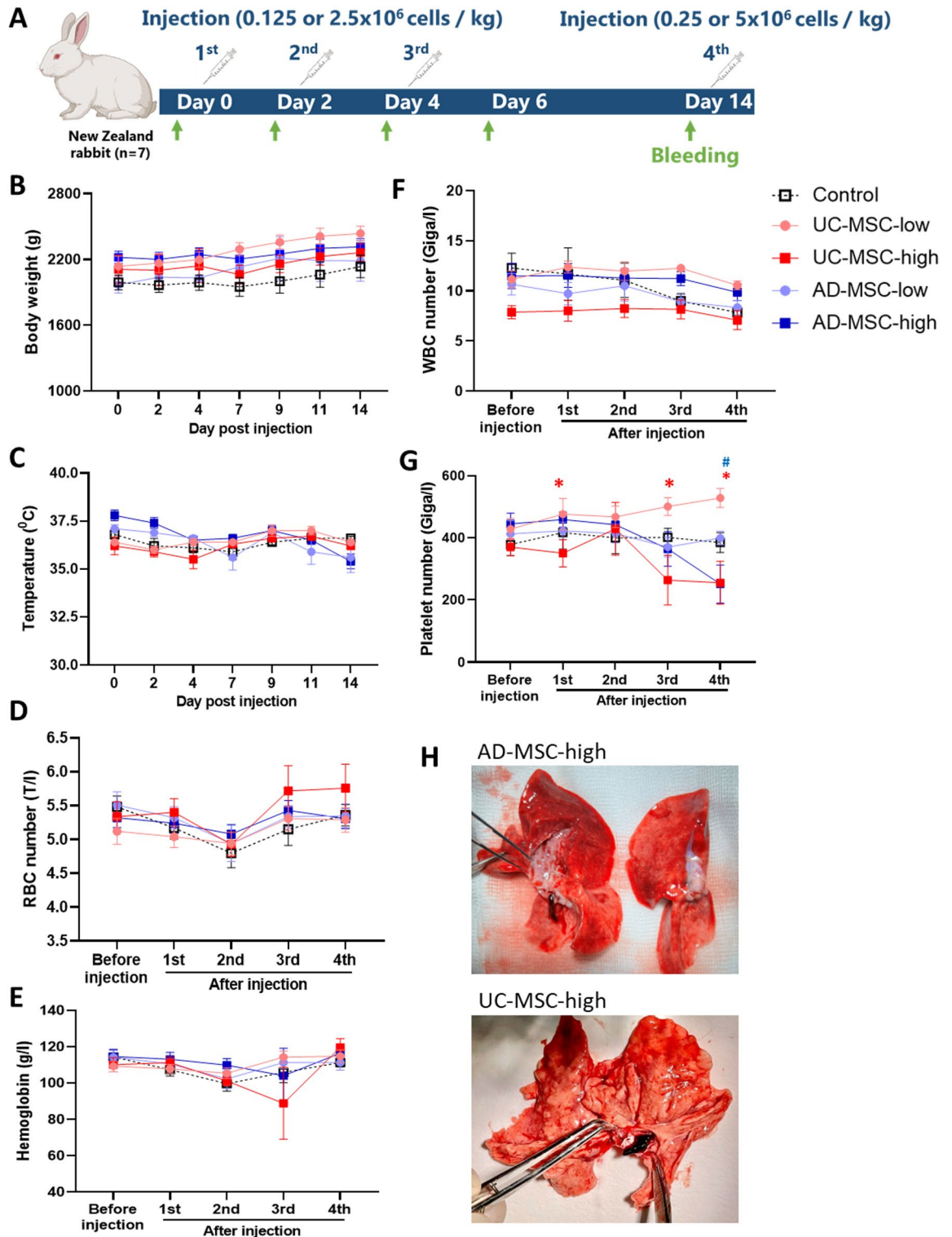


**Fig. 3.** Effects of UC-MSCs and AD-MSCs on hematological parameters in the systemic hypersensitivity test. (A) New Zealand white rabbits were injected with UC-MSCs or AD-MSCs at doses of  $0.125$  or  $2.5 \times 10^6$  cells/kg on days 0, 2, and 4, followed by an additional double dose of  $0.25$  or  $5 \times 10^6$  cells/kg on day 14. The control group received injections of Ringer’s lactate. (B–C) The body weights and body temperatures of the injected animals were monitored for 14 days. (D–G) Peripheral blood was collected from the experimental animals 30 min prior to each injection, as indicated in the experimental diagram (A). RBC (D), hemoglobin (E), WBC (F), and platelet (G) levels were measured. (H) Representative images of thrombosis in the lungs of dead rabbits. Data were presented as mean  $\pm$  SD. p values were determined via t tests (\*,  $p < 0.05$ , indicated the difference between high and low dose of UC-MSC and #,  $P < 0.05$ , indicated the difference between high and low dose of AD-MSC).

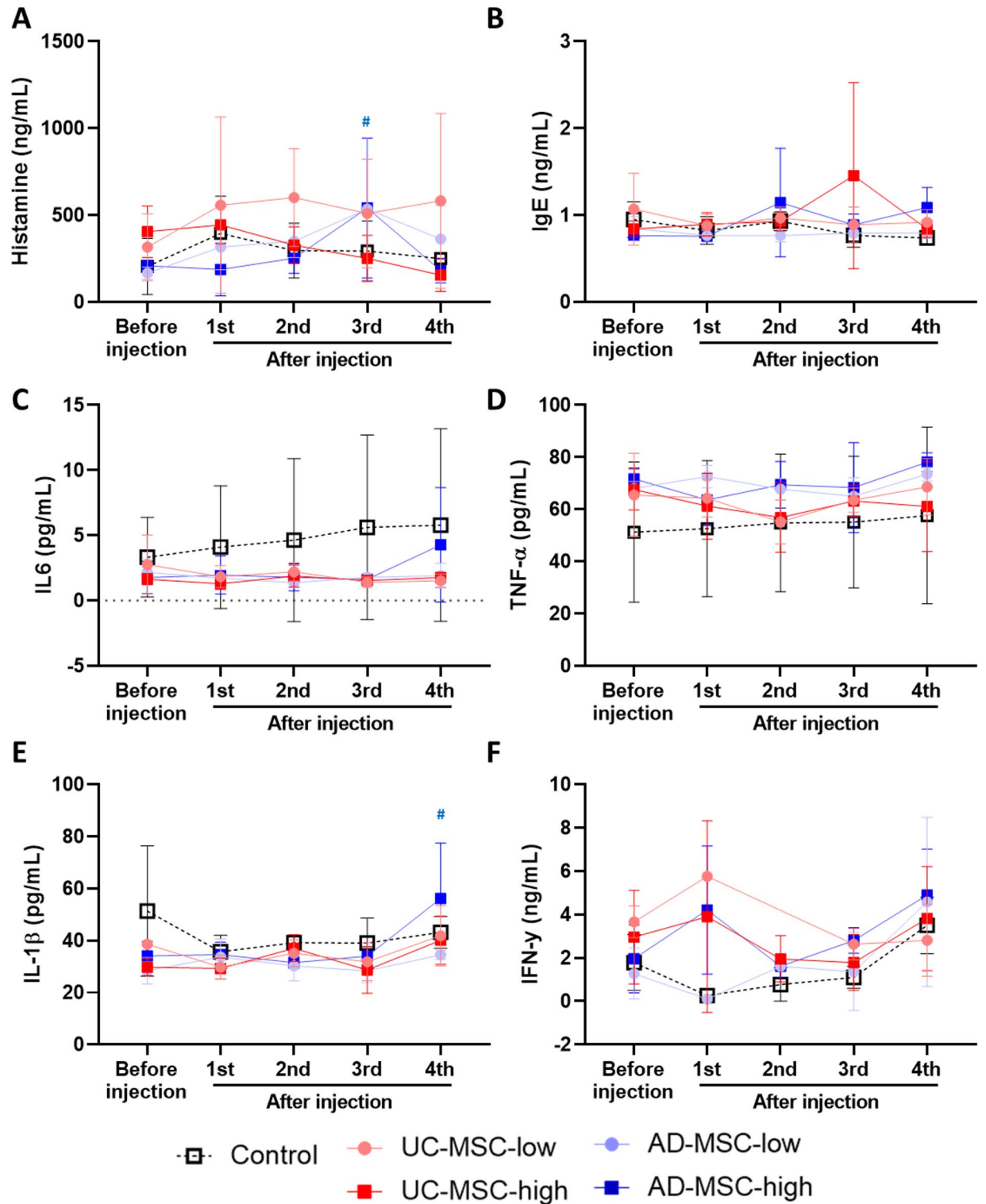


**Fig. 4.** Effects of MSC injection on allergenic and proinflammatory cytokines in the systemic hypersensitivity test. New Zealand white rabbits ( $n=7$ ) were injected with UC-MSCs or AD-MSCs at a dose of  $0.125$  or  $2.5 \times 10^6$  cells/kg on days 0, 2, and 4, followed by an additional double dose of  $0.25$  or  $5 \times 10^6$  cells/kg on day 14. The group injected with Ringer’s lactate served as the control. (A–F) Plasma was obtained from the experimental animals before injection and after the 1st, 2nd, 3rd, and 4th injections. The concentrations of plasma histamine (A), IgE (B), IL-6 (C), IL-1 $\beta$  (D), IFN- $\gamma$  (E), and TNF- $\alpha$  (F) were measured via ELISA. Data were presented as mean  $\pm$  SD.  $p$  values were determined by  $t$  tests (#,  $p < 0.05$ , indicated a difference at the specified time points in AD-MSC-high group).

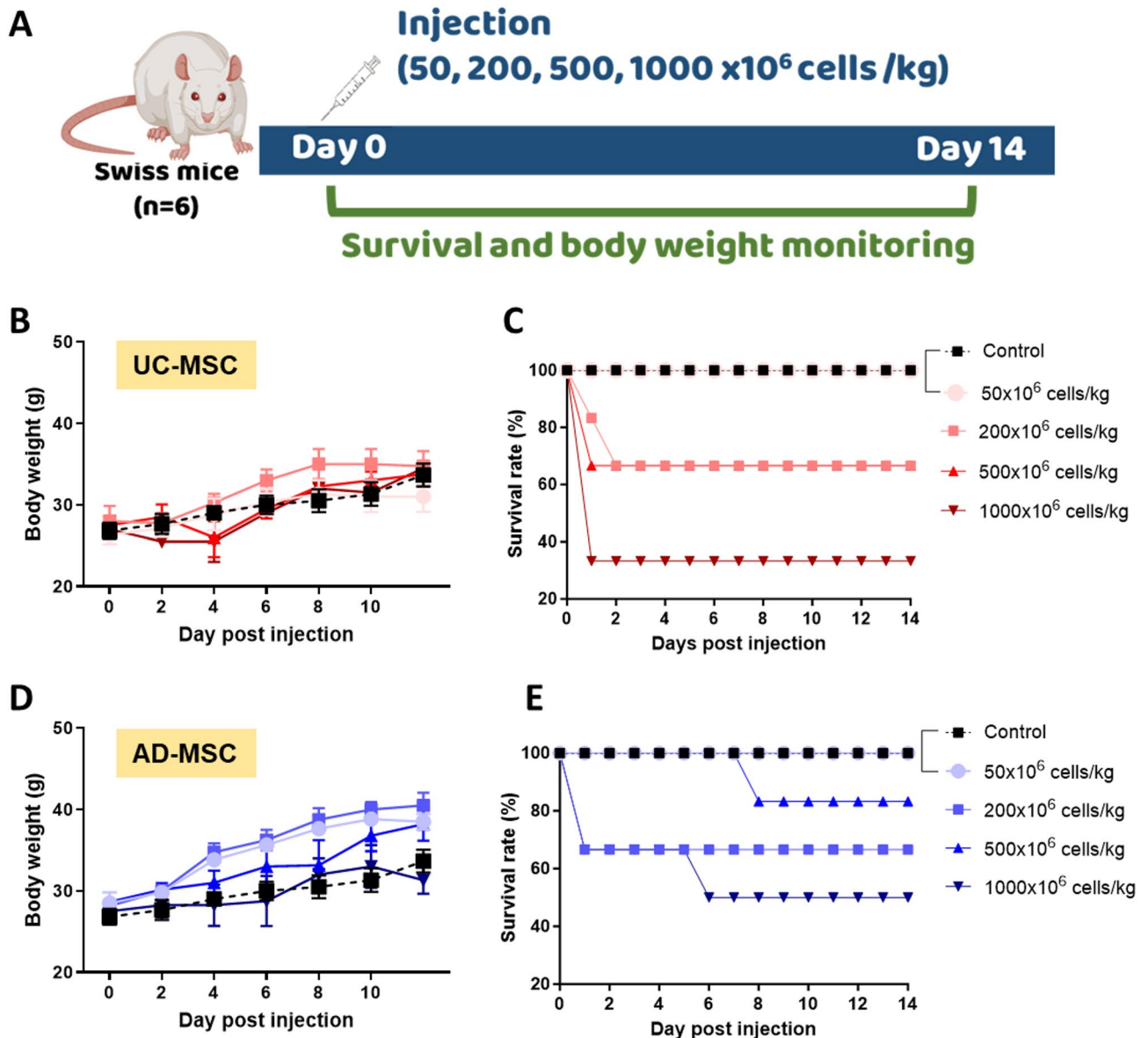


**Fig. 5.** Acute toxicity test of UC-MSCs and AD-MSCs. (A) Swiss mice ( $n=6$ ) were intravenously injected with UC-MSCs or AD-MSCs at doses of 50, 200, 500, or  $1000 \times 10^6$  cells/kg. (B–E) Evaluation of acute toxicity. The body weights (B and D) and mortality rates (C and E) of UC-MSC- and AD-MSC-injected animals were monitored for 14 days. Data were presented as mean  $\pm$  SD.

Figure S1) and AD-MSC (Suppl. Figure S2) groups. LD50 values were then interpolated from these curves as  $575 \times 10^6$  cells/kg for UC-MSCs and  $741 \times 10^6$  cells/kg for AD-MSCs.

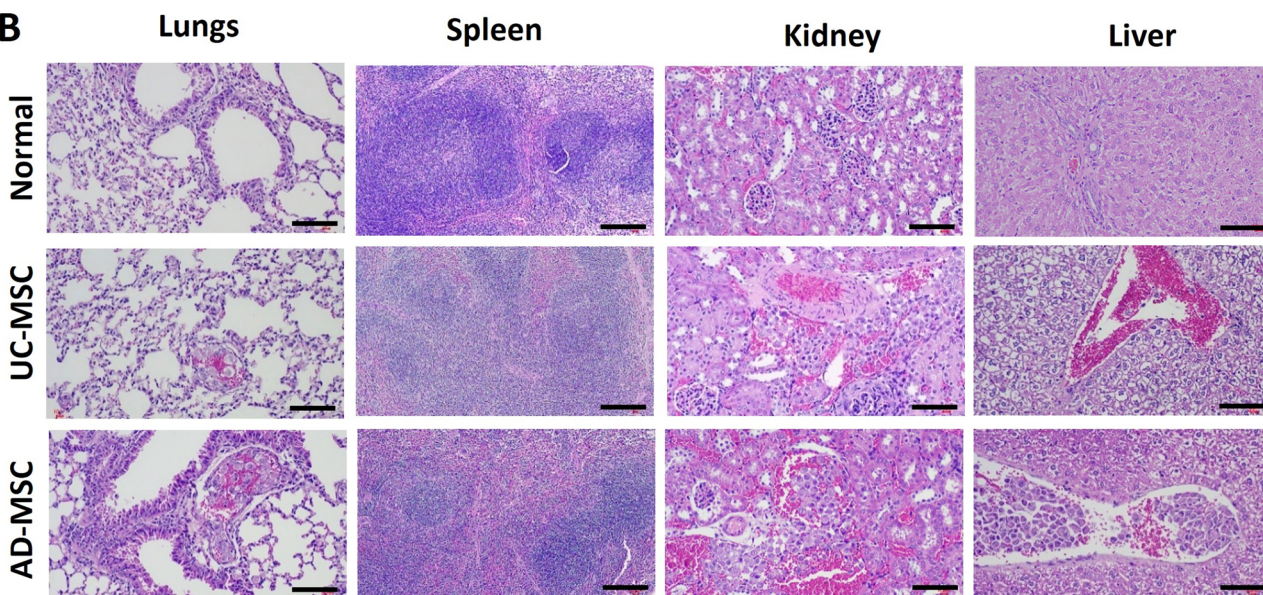
To further investigate the cause of death in the animals, we conducted autopsies and histological examinations of the deceased mice. No abnormalities in the organs of the deceased mice were evident during autopsy. However, images from HE-stained sections revealed the presence of cellular thrombosis in the lungs, kidneys, and liver of these animals (Fig. 6A and B). Cellular thrombosis was frequently detected in the lungs and liver of the mice that were injected with 200, 500, or  $1000 \times 10^6$  cells/kg, whereas it was detected only in the kidneys of the group that was injected with  $1000 \times 10^6$  cells/kg UC-MSCs or AD-MSCs. No cellular thrombosis was observed in the spleens of any of the deceased animals (Fig. 6A). Furthermore, acute liver injury characterized by vacuolar degeneration of hepatocytes was observed in the livers of the MSC-injected groups after injection of the examined doses (Fig. 6A and B). Taken together, our data suggest that the high dose of injected MSCs could induce vascular occlusion in the lungs, kidneys, and liver, as well as acute injury in the liver, leading to the death of mice.

#### Subchronic toxicity of UC-MSC and AD-MSC injection

To investigate the effects of UC-MSCs and AD-MSCs on subchronic toxicity, Wistar rats ( $n=6$  per group) were injected 3 times at 10-day intervals with low ( $5 \times 10^6$  cells/kg) or high ( $15 \times 10^6$  cells/kg) doses of UC-

**A**

Group	Lungs	Spleen	Kidney	Liver
<b>Control</b>	Normal lung parenchyma	Normal splenic parenchyma	Normal renal parenchymal	Normal liver parenchymal
<b>UC-MSC-200</b>	<b>Cellular thrombosis</b>	Normal splenic parenchyma	Normal renal parenchymal	<b>Cellular thrombosis</b> and <b>vacuolar hepatocyte degeneration</b>
<b>UC-MSC-500</b>	<b>Cellular thrombosis</b>	Normal splenic parenchyma	Normal renal parenchymal	<b>Cellular thrombosis</b> and <b>vacuolar hepatocyte degeneration</b>
<b>UC-MSC-1000</b>	<b>Cellular thrombosis</b>	Normal splenic parenchyma	<b>Cellular thrombosis</b>	<b>Cellular thrombosis</b> and <b>vacuolar hepatocyte degeneration</b>
<b>AD-MSC-200</b>	<b>Cellular thrombosis</b>	Normal splenic parenchyma	Normal renal parenchymal	<b>Vacuolar hepatocyte degeneration</b>
<b>AD-MSC-500</b>	Normal lung parenchyma	Normal splenic parenchyma	Normal renal parenchymal	<b>Cellular thrombosis</b> and <b>vacuolar hepatocyte degeneration</b>
<b>AD-MSC-1000</b>	<b>Cellular thrombosis</b>	Normal splenic parenchyma	<b>Cellular thrombosis</b>	<b>Cellular thrombosis</b> and <b>vacuolar hepatocyte degeneration</b>

**B**

**Fig. 6.** Histological analysis of dead mice after testing the acute toxicity of UC-MSCs and AD-MSCs. **(A)** The main organs of the dead animals were sectioned, and HE staining was conducted for histological analysis. **(B)** Representative sections of the lungs, spleen, kidney, and liver showing the tissue structure and the appearance of cellular thrombosis. Scale bars, 100  $\mu$ m.

MSCs or AD-MSCs (Fig. 7A). The body weights of the mice gradually increased, and no significant difference was observed between the experimental groups and the control group during the follow-up period (Fig. 7B). The results of the blood cell count at the indicated time points revealed that neither UC-MSCs nor AD-MSCs affected hematological indices, and the levels of WBCs (Fig. 7C), RBCs (Fig. 7D), hemoglobin (Fig. 7E), or

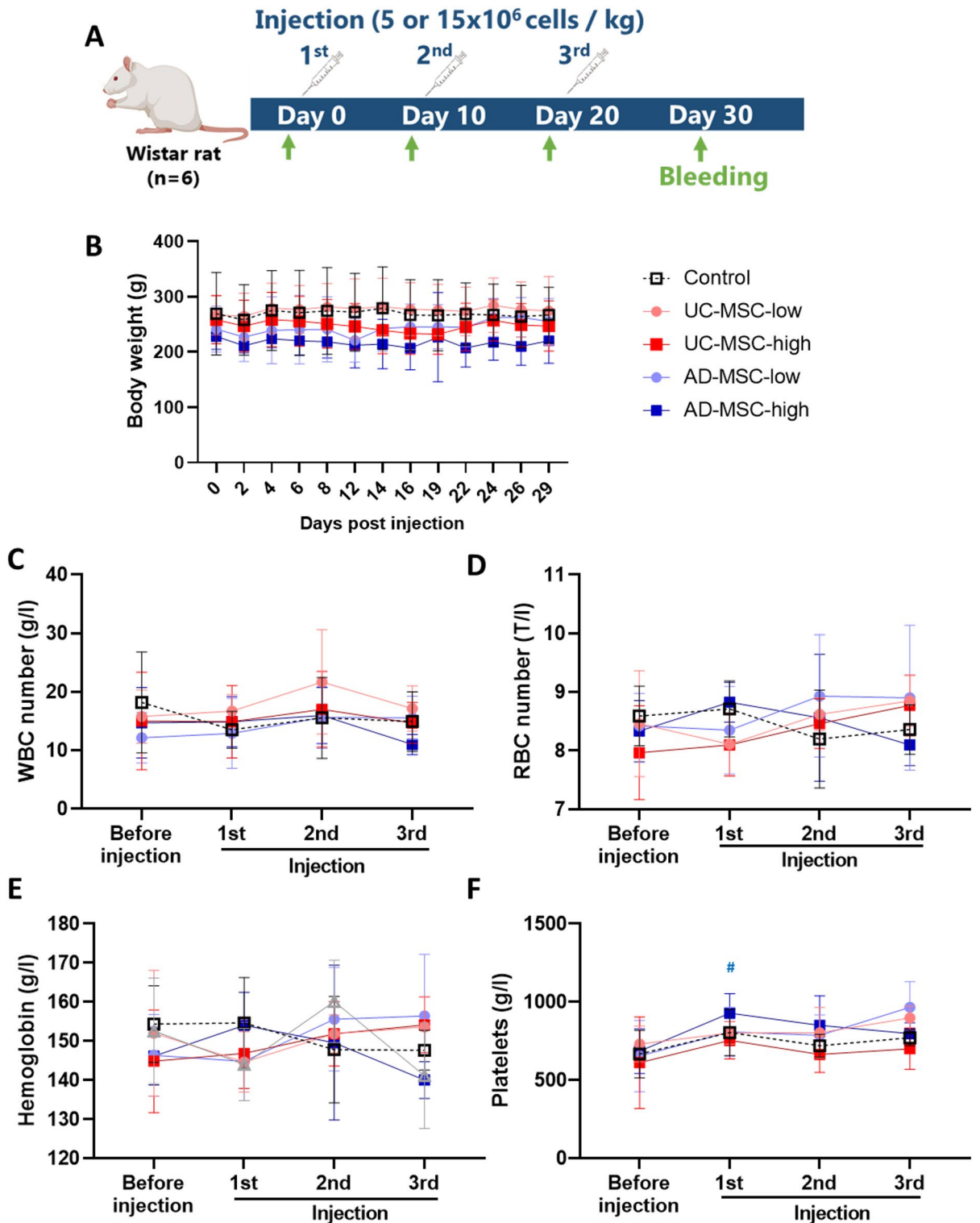


**Fig. 7.** Subchronic toxicity test of UC-MSCs and AD-MSCs. **(A)** Wistar rats ( $n=6$ ) received intravenous injections of either UC-MSCs or AD-MSCs at low ( $5 \times 10^6$  cells/kg) or high ( $15 \times 10^6$  cells/kg) doses on days 0, 10, and 20. The group that was injected with Ringer’s lactate served as the control. **(B)** The body Weights of the injected animals were monitored for 29 days. **(C–F)** Measurement of hematological indices. The levels of WBCs **(C)**, red blood cells **(D)**, hemoglobin **(E)**, and platelets **(F)** were measured in blood samples that were collected at the indicated time points. The data are presented as mean  $\pm$  SD.  $p$  values were determined by  $t$  tests ( $\#$ ,  $p < 0.05$ , indicates the difference at the indicated time point with before injection of high dose of AD-MSC group).

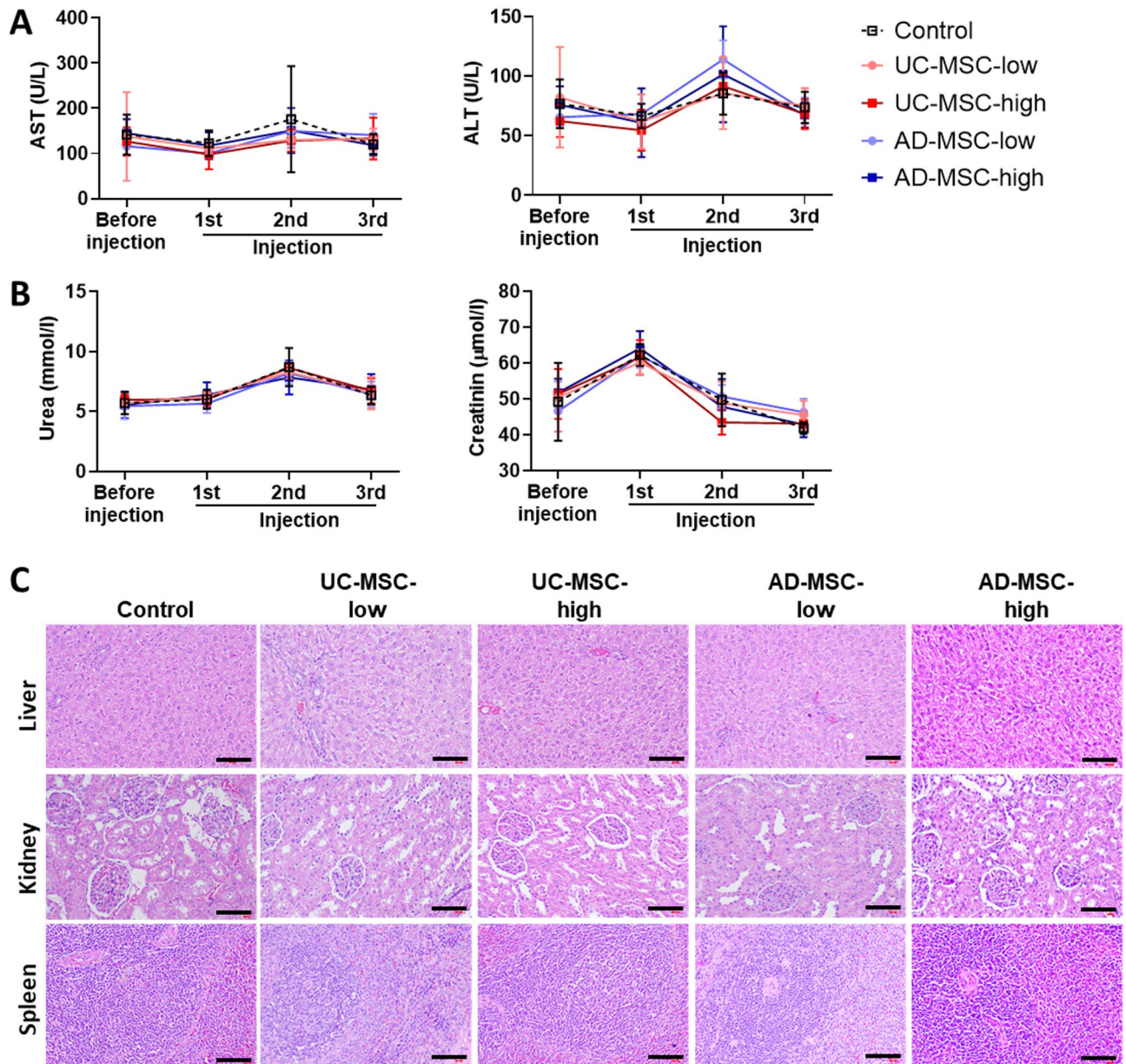


**Fig. 8.** Organ functions in the subchronic toxicity test of UC-MSCs and AD-MSCs. Wistar rats ( $n=6$ ) received intravenous injections of either UC-MSCs or AD-MSCs at low ( $5 \times 10^6$  cells/kg) or high ( $15 \times 10^6$  cells/kg) doses on days 0, 10, and 20. The groups that were injected with Ringer's lactate or left untreated served as controls. The levels of AST and ALT (A) and urea and creatinine (B) in blood samples that were collected before and after each injection were measured. At the termination of the experiment, 50% of the animals in each group ( $n=3$ ) were sacrificed, and the liver, kidney, spleen, and lungs were collected for macroscopic and microscopic observation by H&E staining (C). Scale bars, 100  $\mu$ m.

platelets (Fig. 7F) in the injected rats did not differ from those in the control group. However, an elevated platelet count was noted after the 1st injection compared with the baseline value in the AD-MSC-high group ( $p < 0.05$ ) (Fig. 7F), indicating a potential increased susceptibility to blood clotting in this cohort. In addition, 2 rats in the AD-MSC-high group died after the 1st injection.

Next, liver function was examined by measuring the concentrations of aminotransferase (AST) and alanine aminotransferase (ALT), and kidney function was assessed by measuring the concentrations of urea and creatinine. The data indicated that the levels of AST and ALT (Fig. 8A), as well as those of urea and creatinine (Fig. 8B), did not differ between the injected groups and the control group. Furthermore, no differences in the levels of these parameters were observed before or after the injection in any of the treated groups. Overall, the results suggest that the repeated administration of either UC-MSCs or AD-MSCs did not affect the liver or kidney function of the injected animals. Histological evaluation of major organs, including the liver, kidney, and

spleen, revealed a normal parenchymal structure of these tissues in the injected rats at the termination of the experiment (Fig. 8C).

## Discussion

Hypoxic conditions have been demonstrated to promote the biological activities of MSCs *in vitro*, as these culture conditions reflect the physiological milieu of numerous tissues in the human body<sup>9,12</sup>. Although thorough research has been conducted on the *in vitro* effects of hypoxic MSCs, our understanding of the safety of hypoxic MSCs in animal models is limited. In this study, we comprehensively investigated the safety of hypoxia-primed UC-MSCs and AD-MSCs from various perspectives, such as vascular and muscular stimulation, systemic hypersensitivity, acute toxicity, and subchronic toxicity.

Our data demonstrated that the administration of either UC-MSCs or AD-MSCs did not cause muscular stimulation. Both UC-MSCs and AD-MSCs induced an increase in lesion area and infiltrating cells at the injection site, indicating local tissue inflammation. We suspect that this localized immune response may result from the presence of xenogeneic human cells, as previously reported<sup>35</sup>. However, only the increase observed following UC-MSC administration reached statistical significance. In unpublished data, we analyzed the secretion profiles of 11 cytokines from AD-MSCs and UC-MSCs. Among these, UC-MSCs secreted higher concentrations of IL-6 compared to AD-MSCs. Given that IL-6 is involved in acute phase inflammatory responses<sup>36</sup>, these findings suggest that cytokine-mediated paracrine effects, particularly from IL-6, may underlie the observed tissue reactivity following UC-MSC injection.

MSCs are generally considered poorly immunogenic because of their low expression of MHC/HLA class I and lack of expression of MHC/HLA class II<sup>37</sup>. MSCs also exhibit immunomodulatory effects via the secretion of anti-inflammatory cytokines such as IL-10, IL-6, IL-4, and IL-13<sup>38</sup>. On the other hand, MSCs have been reported to release significant levels of monocyte chemoattractant protein-1 (MCP-1), IL-8, and IL-6 *in vitro*<sup>39–41</sup>. In the animals in which systemic hypersensitivity was analyzed, the levels of histamine, IL-1 $\beta$ , and IFN- $\gamma$  increased after MSC injection compared with those at baseline (before injection) in the high-dose AD-MSC group but not in the high-dose UC-MSC group. Although this increase was not statistically significant compared with that of the control group and was thus considered toxicologically insignificant, the data might suggest that AD-MSCs were likely more immunogenic than UC-MSCs were. The source of MSCs may contribute to their differing immunogenic characteristics<sup>37</sup>. Research by Tan et al.<sup>42</sup> revealed that UC-MSCs express fewer MHC class I molecules and IFN- $\gamma$  receptors than AD-MSCs do, indicating that, compared with UC-MSCs, AD-MSCs have greater immunogenicity.

Repeated intravenous injections of UC-MSCs or AD-MSCs did not affect the hematopoietic functions of rabbits or Wistar rats, as indicated by the normal RBC, hemoglobin, and WBC levels. In addition, the injected mice exhibited no significant changes in the function or histological structure of the liver, kidney, or spleen in the subchronic toxicity test. However, repeated injections of a high dose of both AD-MSCs and UC-MSCs ( $2.5 \times 10^6$  cells/kg three times and  $5 \times 10^6$  cells/kg at the 4th injection) were associated with a risk of platelet alterations and vascular thrombosis development in the systemic hypersensitivity test. We noted a decreased platelet count in animals that received high MSC doses compared with those that received lower doses. A decreased platelet count (thrombocytopenia) has been reported to be involved in disseminated intravascular coagulation (DIC), which is a condition that is triggered by excessive thrombus formation inside blood vessels<sup>43</sup>. In DIC, the excessive consumption of platelets at the clotting site leads to a sharp decrease in their number in peripheral blood. From this perspective, the significant decrease in the platelet number in the high-dose MSC groups may indicate severe clot formation in the lungs of the experimental animals, potentially causing animal death. In particular, 2 of 7 and 3 of 7 rabbits died after receiving high doses of UC-MSCs and AD-MSCs, respectively, probably due to pulmonary thrombosis.

Our investigation of the lethal effects of increasing doses of UC-MSCs and AD-MSCs revealed that a dose of  $50 \times 10^6$  cells/kg did not induce abnormal behaviors in mice. Therefore, doses below this level are considered safe for systemic infusion. This dose is equivalent to the maximal nonlethal intravenous dose of BM-MSCs in mice that was reported by Giri et al.<sup>44</sup>. When converted to a human dose (with a conversion ratio of 0.081<sup>45</sup>,  $50 \times 10^6$  cells/kg equates to a Human dose of approximately  $4 \times 10^6$  cells/kg, which is four times greater than the common clinical dose for intravenous infusion of  $1 \times 10^6$  cells/kg<sup>46</sup>. The intravenous injection of UC-MSCs or AD-MSCs at  $200\text{--}1000 \times 10^6$  cells/kg induced the death of the mice, resulting in LD50 values of  $575 \times 10^6$  cells/kg and  $741 \times 10^6$  cells/kg for UC-MSCs and AD-MSCs, respectively (equivalent to a Human dose of approximately  $46 \times 10^6$  cells/kg and  $60 \times 10^6$  cells/kg, respectively). The experimental animals died within 2–30 min after MSC injection and experienced severe symptoms, including dyspnea, cyanosis, tetraplegia, coolness of the extremities, exophthalmos, and respiratory failure. Similar adverse effects on mice were described by Liao et al. after infusing  $3\text{--}4 \times 10^6$  mouse BM-derived MSCs per head (corresponding to  $150\text{--}200 \times 10^6$  cells/kg, considering mice Weighing 20 g)<sup>47</sup>. Additionally, we detected cellular thrombi in the lungs, kidneys, and livers of dead mice after MSC injection, and the results were consistent with observations from previous studies. Tatsumi et al. observed microthrombi in the lungs and hearts of mice after intravenous administration of  $1.5 \times 10^6$  mouse AD-MSCs per mouse (corresponding to  $75 \times 10^6$  cells/kg, considering mice Weighing 20 g)<sup>48</sup>. Oeller et al. observed intravascular thromboembolism in the lungs, spleen, and Liver of rats after intravenous injection of  $6 \times 10^6$  cells/kg human UC-MSCs<sup>49</sup>. The interaction of infused MSCs with blood is well known to initiate coagulation and subsequently cause thrombosis in animal models<sup>47</sup> and patients who receive MSCs in clinical trials<sup>50–52</sup>. Our group demonstrated that high expression of tissue factors on UC-MSCs and AD-MSCs that were cultured under SF/XF conditions was associated with high coagulant activity<sup>53</sup>. Notably, acute liver injury characterized by vacuolar degeneration of hepatocytes was observed in HE-stained sections from all the dead mice. This might occur due to thrombogenesis events. The formation of intravascular thrombi could reduce the oxygen supply to the tissue<sup>54</sup>. Under decreased oxygen conditions, mitochondria produce less ATP, impairing the activity of

Na<sup>+</sup>/K<sup>+</sup> ATPase pumps in the cell membrane. This impairment causes passive entry of Na<sup>+</sup>, followed by water, to maintain osmotic balance<sup>55</sup>, leading to the vacuolar degeneration observed in the liver. Taken together, our results indicate that prophylactic intervention with anticoagulant drugs to control intravascular thrombosis might improve the safety of MSC infusion.

## Conclusion

Our comprehensive study confirms the preliminary safety of hypoxic MSCs and provides initial proof-of-concept that transplantation of hypoxic MSCs is an effective and safe cell-based therapy for disease treatment. Our findings demonstrate that hypoxic MSCs are well tolerated at a dose that is considerably higher than the dose that is typically used for clinical therapy, indicating a strong safety profile. The determined tolerated dose and LD50 values of hypoxic MSCs offer a valuable starting point for establishing appropriate doses for preclinical investigations and for determining therapeutic doses for clinical applications. As large animals, such as sheep, pigs, and nonhuman primates, are more anatomically and physiologically comparable to humans, we suggest that further assessments of safety, efficacy, and dosing in other animal models should be performed to support the clinical translation of hypoxic MSC-based therapy.

## Data availability

Data are provided within the manuscript or supplementary information files.

Received: 31 December 2024; Accepted: 11 September 2025

Published online: 15 October 2025

## References

- Ullah, I., Subbarao, R. B. & Rho, G. J. Human mesenchymal stem cells - current trends and future prospective. *Biosci. Rep.* **35** (2), e00191 (2015).
- Marion, N. W. & Mao, J. J. Mesenchymal stem cells and tissue engineering. *Methods Enzymol.* **420**, 339–361 (2006).
- Selich, A. et al. Umbilical cord as a long-term source of activatable mesenchymal stromal cells for Immunomodulation. *Stem Cell Res. Ther.* **10** (1), 285 (2019).
- Marquez-Curtis, L. A., Janowska-Wieczorek, A., McGann, L. E. & Elliott, J. A. W. Mesenchymal stromal cells derived from various tissues: biological, clinical and cryopreservation aspects. *Cryobiology* **71** (2), 181–197 (2015).
- Berebichez-Fridman, R. & Montero-Olvera, P. R. Sources and clinical applications of mesenchymal stem cells. *Sultan Qaboos Univ. Med. J.* **18** (3), e264–e277 (2018).
- Han, Y. et al. Mesenchymal stem cells for regenerative medicine. *Cells* **8** (8), 886 (2019).
- Cheung, T. S. et al. Mesenchymal stromal cells for graft versus host disease: mechanism-based biomarkers. *Front. Immunol.* **11**, 1338 (2020).
- Rehman, A. et al. Mesenchymal stem cells in soft tissue regenerative medicine: a comprehensive review. *Med. (Mex)*. **59** (8), 1449 (2023).
- Antebi, B. et al. Short-term physiological hypoxia potentiates the therapeutic function of mesenchymal stem cells. *Stem Cell Res. Ther.* **9** (1), 265 (2018).
- Pulido-Escribano, V. et al. Role of hypoxia preconditioning in therapeutic potential of mesenchymal stem-cell-derived extracellular vesicles. *World J. Stem Cells*. **14** (7), 453–472 (2022).
- Widowati, W. et al. Hypoxia in mesenchymal stem cell. in: hypoxia and human diseases [internet]. IntechOpen; [cited 2024 Feb 17]. (2017). Available from: <https://www.intechopen.com/chapters/52644>
- The hematopoietic stem cell niche: low in oxygen but a nice place to be - PubMed [Internet]. [cited 2024 Aug 12]. Available from: <https://pubmed.ncbi.nlm.nih.gov/19725055/>
- Eliasson, P. & Jönsson, J. I. The hematopoietic stem cell niche: low in oxygen but a nice place to be. *J. Cell. Physiol.* **222** (1), 17–22 (2010).
- Haque, N., Rahman, M. T., Abu Kasim, N. H. & Alabsi, A. M. Hypoxic culture conditions as a solution for mesenchymal stem cell based regenerative therapy. *Sci. World J.* **2013**, 1–12 (2013).
- Spencer, J. A. et al. Direct measurement of local oxygen concentration in the bone marrow of live animals. *Nature* **508** (7495), 269–273 (2014).
- Widowati, W. et al. Effect of oxygen tension on proliferation and characteristics of wharton's jelly-derived mesenchymal stem cells. *Biomark. Genomic Med.* **6** (1), 43–48 (2014).
- Kwon, S. Y. et al. Hypoxia enhances cell properties of human mesenchymal stem cells. *Tissue Eng. Regen Med.* **14** (5), 595–604 (2017).
- Li, B. et al. Hypoxia-induced mesenchymal stromal cells exhibit an enhanced therapeutic effect on radiation-induced lung injury in mice due to an increased proliferation potential and enhanced antioxidant ability. *Cell. Physiol. Biochem. Int. J. Exp. Cell. Physiol. Biochem. Pharmacol.* **44** (4), 1295–1310 (2017).
- Hu, X. et al. Transplantation of hypoxia-preconditioned mesenchymal stem cells improves infarcted heart function via enhanced survival of implanted cells and angiogenesis. *J. Thorac. Cardiovasc. Surg.* **135** (4), 799–808 (2008).
- Almeria, C. et al. Hypoxia conditioned mesenchymal stem cell-derived extracellular vesicles induce increased vascular tube formation in vitro. *Front. Bioeng. Biotechnol.* **7**, 292 (2019).
- Noronha, N. C. et al. Hypoxia priming improves in vitro angiogenic properties of umbilical cord derived-mesenchymal stromal cells expanded in stirred-tank bioreactor. *Biochem. Eng. J.* **168**, 107949 (2021).
- Li, H., Dai, H. & Li, J. Immunomodulatory properties of mesenchymal stromal/stem cells: the link with metabolism. *J. Adv. Res.* **45**, 15–29 (2022).
- Jiang, C. M. et al. Effects of hypoxia on the Immunomodulatory properties of human gingiva-derived mesenchymal stem cells. *J. Dent. Res.* **94** (1), 69–77 (2015).
- Roemeling-Van Rhijn, M. et al. Effects of hypoxia on the immunomodulatory properties of adipose tissue-derived mesenchymal stem cells. *Front Immunol* [Internet]. [cited 2024 Feb 17];4. Available from: <https://www.frontiersin.org/journals/immunology/articles/2013>. <https://doi.org/10.3389/fimmu.2013.00203>
- Alagesan, S. et al. Enhancement strategies for mesenchymal stem cells and related therapies. *Stem Cell Res. Ther.* **13**, 75 (2022).
- Wei, L., Fraser, J. L., Zhong-Yang, L., Hu, X. & Yu, S. P. Transplantation of hypoxia preconditioned bone marrow mesenchymal stem cells enhances angiogenesis and neurogenesis after cerebral ischemia in rats. *Neurobiol. Dis.* **46** (3), 635–645 (2012).
- Kojima, Y. et al. Mesenchymal stem cells cultured under hypoxic conditions had a greater therapeutic effect on mice with liver cirrhosis compared to those cultured under normal oxygen conditions. *Regen Ther.* **11**, 269–281 (2019).

28. Lan, Y. W. et al. Hypoxia-preconditioned mesenchymal stem cells attenuate bleomycin-induced pulmonary fibrosis. *Stem Cell. Res. Ther.* **6** (1), 97 (2015).
29. Horie, S. et al. Cytokine pre-activation of cryopreserved xenogeneic-free human mesenchymal stromal cells enhances resolution and repair following ventilator-induced lung injury potentially via a KGF-dependent mechanism. *Intensive Care Med. Exp.* **8** (1), 8 (2020).
30. Liu, S., Yang, W., Li, Y. & Sun, C. Fetal bovine serum, an important factor affecting the reproducibility of cell experiments. *Sci. Rep.* **13**, 1942 (2023).
31. Subbiahanadar Chelladurai, K. et al. Alternative to FBS in animal cell culture - An overview and future perspective. *Heliyon* **7** (8), e07686 (2021).
32. Hoang, V. T. et al. Standardized xeno- and serum-free culture platform enables large-scale expansion of high-quality mesenchymal stem/stromal cells from perinatal and adult tissue sources. *Cytotherapy* **23** (1), 88–99 (2021).
33. Safety evaluation of exosomes. derived from human umbilical cord mesenchymal stromal cell - PubMed [Internet]. [cited 2024 May 7]. Available from: <https://pubmed.ncbi.nlm.nih.gov/26857231/>
34. Dominici, M. et al. Minimal criteria for defining multipotent mesenchymal stromal cells. The international society for cellular therapy position statement. *Cytotherapy* **8** (4), 315–317 (2006).
35. Riestter, S. M. et al. Safety studies for use of adipose tissue-derived mesenchymal stromal/stem cells in a rabbit model for osteoarthritis to support a phase I clinical trial. *Stem Cells Transl Med.* **6** (3), 910–922 (2017).
36. Tanaka, T., Narazaki, M. & Kishimoto, T. IL-6 in inflammation, immunity, and disease. *Cold Spring Harb Perspect. Biol.* **6** (10), a016295 (2014).
37. Chen, W., Lv, L., Chen, N. & Cui, E. Immunogenicity of mesenchymal stromal/stem cells. *Scand. J. Immunol.* **97** (6), e13267 (2023).
38. Kyurkchiev, D. et al. Secretion of immunoregulatory cytokines by mesenchymal stem cells. *World J. Stem Cells.* **6** (5), 552–570 (2014).
39. Peshkova, M. et al. MSCs' conditioned media cytokine and growth factor profiles and their impact on macrophage polarization. *Stem Cell. Res. Ther.* **14** (1), 142 (2023).
40. Ngo, A. T. L. et al. Clinically relevant preservation conditions for mesenchymal stem/stromal cells derived from perinatal and adult tissue sources. *J. Cell. Mol. Med.* **25** (22), 10747–10760 (2021).
41. Park, C. W. et al. Cytokine secretion profiling of human mesenchymal stem cells by antibody array. *Int. J. Stem Cells.* **2** (1), 59–68 (2009).
42. Tan, K. et al. Impact of adipose tissue or umbilical cord derived mesenchymal stem cells on the immunogenicity of human cord blood derived endothelial progenitor cells. *PLoS ONE.* **12** (5), e0178624 (2017).
43. Santoshi, R. K., Patel, R., Patel, N. S., Bansro, V. & Chhabra, G. A comprehensive review of thrombocytopenia with a spotlight on intensive care patients. *Cureus* **14**(8), e27718 (2022).
44. Giri, J. & Galipeau, J. Mesenchymal stromal cell therapeutic potency is dependent upon viability, route of delivery, and immune match. *Blood Adv.* **4** (9), 1987–1997 (2020).
45. Nair, A. B. & Jacob, S. A simple practice guide for dose conversion between animals and human. *J. Basic. Clin. Pharm.* **7** (2), 27–31 (2016).
46. Lin, Y. & Hogan, W. J. Clinical application of mesenchymal stem cells in the treatment and prevention of graft-versus-host disease. *Adv. Hematol.* **2011**, 427863 (2011).
47. Liao, L. et al. Heparin improves BMSC cell therapy: anticoagulant treatment by heparin improves the safety and therapeutic effect of bone marrow-derived mesenchymal stem cell cytotreatment. *Theranostics* **7** (1), 106–116 (2017).
48. Tatsumi, K. et al. Tissue factor triggers procoagulation in transplanted mesenchymal stem cells leading to thromboembolism. *Biochem. Biophys. Res. Commun.* **431** (2), 203–209 (2013).
49. Oeller, M. et al. Selection of tissue factor-deficient cell transplants as a novel strategy for improving hemocompatibility of human bone marrow stromal cells. *Theranostics* **8** (5), 1421–1434 (2018).
50. Jung, J. W. et al. Familial occurrence of pulmonary embolism after intravenous, adipose tissue-derived stem cell therapy. *Yonsei Med. J.* **54** (5), 1293–1296 (2013).
51. Wang, H. et al. Autologous mesenchymal stem cell and islet cotransplantation: safety and efficacy. *Stem Cells Transl Med.* **7** (1), 11–19 (2017).
52. Wu, Z. et al. Thromboembolism induced by umbilical cord mesenchymal stem cell infusion: a report of two cases and literature review. *Transpl. Proc.* **49** (7), 1656–1658 (2017).
53. Impact of tissue factor. expression and administration routes on thrombosis development induced by mesenchymal stem/stromal cell infusions: re-evaluating the dogma - PMC [Internet]. [cited 2024 Apr 1]. Available from: <https://www.ncbi.nlm.nih.gov/pmc/articles/PMC10900728/>
54. Ashorobi, D., Ameer, M. A. & Fernandez, R. Thrombosis. In: StatPearls [Internet] [Internet]. StatPearls Publishing; [cited 2024 Jun 6]. (2024). Available from: <https://www.ncbi.nlm.nih.gov/books/NBK538430/>
55. Gusarova, G. A. et al. Hypoxia leads to Na,K-ATPase downregulation via Ca<sup>2+</sup> Release-Activated Ca<sup>2+</sup> Channels and AMPK activation  $\nabla$ . *Mol. Cell. Biol.* **31** (17), 3546–3556 (2011).

## Author contributions

Nhung Thi-Hong Dinh, Quyen Thi Nguyen and Ngo Thu Hang, : Conceptualization, Data curation, Formal analysis, Investigation, Methodology, Validation, Visualization, Writing – original draft, Writing – review & editing; Can Van Mao, and Xuan-Hai Do: Investigation, Methodology, Validation, Visualization; Le Duc Son, Hong-Nhung Dao, and Giang Trang Ngan: Data analysis, Investigation; Van T. Hoang and Liem Nguyen Thanh: Conceptualization, Methodology, Supervision, Validation, Visualization, Writing – review & editing.

## Funding

This work is supported by the Vingroup Scientific Research Grant (Project number: PRO2178).

## Declarations

## Competing interests

The authors declare no competing interests.

## Ethics approval

Ethics approval was obtained from the Ethical Committee of Vinmec International Hospital (approval No.18/2022/CN-HĐĐĐ VMEC, dated 9th March 2022) and Dinh Tien Hoang Institute of Medicine, Vietnam (approval no. IRB-A-2201, dated 5th June 2022).

### Consent to participate

Informed consent was obtained from all subjects prior to the collection of adipose tissue or umbilical cord samples.

### Consent to publish

All participants who voluntarily donated adipose tissue or umbilical cord provided written informed consent, agreeing to the use of their biological samples and associated data for research and publication purposes.

### Additional information

**Supplementary Information** The online version contains supplementary material available at <https://doi.org/10.1038/s41598-025-20018-5>.

**Correspondence** and requests for materials should be addressed to V.T.H. or L.N.T.

**Reprints and permissions information** is available at [www.nature.com/reprints](http://www.nature.com/reprints).

**Publisher's note** Springer Nature remains neutral with regard to jurisdictional claims in published maps and institutional affiliations.

**Open Access** This article is licensed under a Creative Commons Attribution-NonCommercial-NoDerivatives 4.0 International License, which permits any non-commercial use, sharing, distribution and reproduction in any medium or format, as long as you give appropriate credit to the original author(s) and the source, provide a link to the Creative Commons licence, and indicate if you modified the licensed material. You do not have permission under this licence to share adapted material derived from this article or parts of it. The images or other third party material in this article are included in the article's Creative Commons licence, unless indicated otherwise in a credit line to the material. If material is not included in the article's Creative Commons licence and your intended use is not permitted by statutory regulation or exceeds the permitted use, you will need to obtain permission directly from the copyright holder. To view a copy of this licence, visit <http://creativecommons.org/licenses/by-nc-nd/4.0/>.

© The Author(s) 2025, corrected publication 2026